Vesicle-Bound Conformation of Melittin: Transferred Nuclear Overhauser Enhancement Analysis in the Presence of Perdeuterated Phosphatidylcholine Vesicles†

Akihiko Okada,‡ Kaori Wakamatsu,*,§ Tatsuo Miyazawa,‖ and Tsutomu Higashijima⊥

Tsukuba Research Laboratory, Sumitomo Chemical Company, Ltd., Kitahara 6, Tsukuba, Ibaraki 300-32, Japan, Faculty of Engineering, Gunma University, Kiryu, Gunma 376, Japan, Protein Engineering Research Institute, Furuedai, Suita, Osaka 565, Japan, and Department of Pharmacology, University of Texas Southwestern Medical Center at Dallas, 5323 Harry Hines Boulevard, Dallas, Texas 75235-9041

Received April 11, 1994; Revised Manuscript Received June 2, 1994®

ABSTRACT: We determined a detailed conformation of the honeybee venom peptide melittin when bound to phosphatidylcholine vesicles using proton NMR. In the presence of vesicles of perdeuterated dipalmitoylglycerophosphocholine, two-dimensional transferred nuclear Overhauser enhancement (TRNOE) experiments were carried out. By a distance geometry calculation using NOE-derived distance constraints followed by a simulated annealing refinement, the N-terminal (Leu^6-Leu^{10}) and C-terminal (Leu^{13}-Lys^{21}) parts were found to have an α-helical conformation, whereas five C-terminal residues (Arg^{22}-Gln^{26}) did not show a unique conformation in the vesicle-bound state. The two α-helices were connected via a less structured segment (Thr^{11}-Gly^{12}) with a helix bend angle of 86° ± 34°. Model distance geometry calculations using distance constraints extracted from a tetrameric melittin molecule in crystal assured us that the NOE constraints can accurately reproduce melittin's structure, as well as helping to interpret the NMR structures. Although the vesicle-bound conformation of melittin is similar to that occurring in a methanol solution and in dodecylphosphocholine micelles, significant differences were found in the conformation of C-terminal basic residues and the helix bend angle. This is the first study to clearly demonstrate conformation differences in micelle- and vesicle-bound peptides. In addition, lytic activity of melittin and its analogs showed better correlation with a peptide conformation in vesicles than in either methanol or micelles.

Melittin is the major constituent of honeybee (*Apis mellifera*) venom, comprising 50% of its dry weight and being a hexacosapeptide with a primary structure of Gly-Ile-Gly-Ala-Val-Leu-Lys-Val-Leu-Thr-Thr-Gly-Leu-Pro-Ala-Leu-Ile-Ser-Trp-Ile-Lys-Arg-Lys-Arg-Gln-Gln-NH_2 [Habermann & Jentsch, 1967; for review, see Habermann (1972), Hider (1988), and Dempsey (1990)]. This particular sequence has two remarkable features in that it has six positive charges and no negative ones, and the N-terminal part (Gly^1-Ile^{20}) is hydrophobic as a whole, whereas the C-terminal part (Lys^{21}-Gln^{26}) is hydrophilic. Melittin possesses various biological activities (Habermann, 1972), i.e., it causes hemolysis, increases ion permeability through native biological membranes or synthetic phospholipid bilayers, and uncouples oxidation from phosphorylation. The peptide also activates endogenous phospholipase A_2 (Mollay & Kreil, 1974) and activates adenylate cyclase at low concentration, while inhibiting it at high concentration (Lad & Schier, 1980). Binding with lipid membranes in conjunction with a simultaneous perturbation in the bilayer structure are considered to be responsible for these activities. Interaction of the peptide with phospholipids has been extensively studied to elucidate the action mechanisms of melittin molecules [see Dempsey (1990) for a review]. In addition, to gain insights into protein–membrane interactions, this peptide has also attracted research interest as a low-molecular-weight model of membrane proteins.

We believe that a detailed conformation of melittin molecules in the membrane-bound state must be known in order to further uncover its activity mechanisms. Although analyses using CD[1] spectroscopy showed that melittin molecules are largely in an α-helical conformation when bound to phospholipid vesicles (Vogel, 1981), detailed information on individual residues cannot be obtained by this method. Conventional high-resolution ^1H NMR spectroscopy is very powerful for determining a detailed molecular conformation in solution, yet it cannot be directly applied to membrane-bound peptide molecules; i.e., the proton signals from such a peptide are too broad to be observed with high resolution due to the slow tumbling motion of peptide molecules while in this state. To avoid broadening of the proton signals, Brown et al. (1982), or more recently, Inagaki et al. (1989), analyzed the conformation of melittin molecules bound to lipid micelles rather than to a lipid bilayer. By distance geometry calculations using NOE-derived constraints, micelle-bound molecules were found to possess two α-helical parts, which were also

† This research was partly supported by the International Scientific Research Program (Joint Research; K.W. and T.H.) and by a US Public Health Service Grant (GM40676; T.H.).

* To whom correspondence should be addressed.

‡ Sumitomo Chemical Co., Ltd.

§ Gunma University.

‖ Protein Engineering Research Institute, passed away on April 30, 1993.

⊥ University of Texas Southwestern Medical Center at Dallas, passed away on June 15, 1993.

® Abstract published in *Advance ACS Abstracts,* July 15, 1994.

[1] Abbreviations: 2D, two dimensional; CD, circular dichroism; CM, carboxymethyl; DPPC-d_{80}, perdeuterated dipalmitoylglycerophosphocholine; HPLC, high-performance liquid chromatography; NMR, nuclear magnetic resonance; NOE, nuclear Overhauser enhancement; NOESY, NOE correlation spectroscopy; ODS, octadecylsilane; PC, phosphatidylcholine; RMSD, root mean square deviation; ROE, rotating frame NOE; ROESY, ROE correlation spectroscopy; TOCSY, total correlation spectroscopy; TPPI, time-proportional phase increment; TRNOE, transferred NOE.

0006-2960/94/0433-9438$04.50/0

found to exist in the crystal structure of melittin tetramer (Terwilliger & Eisenberg, 1982). However, a possibility remains that peptides take different conformations in micelles and vesicles.

We previously showed that the conformation of a peptide molecule bound to a lipid bilayer can be analyzed in detail (Wakamatsu et al., 1983) by applying TRNOE (Albrand et al., 1979; Clore & Gronenborn, 1982; Campbell & Sykes, 1991). More recently, we determined the precise conformation of bilayer-bound mastoparan-X by the combined use of distance geometry and restrained molecular dynamics calculations based on TRNOE constraints (Wakamatsu et al., 1992). Here, we describe the conformation of melittin in the vesicle-bound state based on TRNOE analyses. We found that the resultant conformation in the vesicle-bound state can better explain the activity of melittin and its analogs than does its conformation in the micelle-bound state.

EXPERIMENTAL PROCEDURES

Sample Preparation. Melittin was purified from lyophilized bee venom (grade IV, Sigma) according to King et al. (1976) using G-50 (Pharmacia, Uppsala, Sweden) gel filtration and CM cellulose (Whatman, Kent, England) ion-exchange chromatographies. Gel filtration chromatography completely removed the melittin formylated at the N-terminus. Subsequent analysis of the sample by reversed-phase HPLC with a YMC A-312 (ODS) column (size: 6 × 150 mm; Shimakyu Osaka) using 40% acetonitrile in 0.1% trifluoroacetic acid as an eluate showed the presence of three kinds of impurities. Similar analysis of purified melittin purchased from Sigma (St. Louis, MO) contained the same impurities. Consequently, the derived sample was further fractionated with a YMC S-343 (ODS) column (size: 20 × 250 mm) using 39% acetonitrile in 0.1% trifluoroacetic acid. The purity of each resultant fraction was determined with a YMC A-312 column. The purified fractions were then collected, evaporated, and repeatedly lyophilized to remove the trifluoroacetic acid.

DPPC-d_{80} was chemically synthesized according to Kingsley and Feigenson (1979) with several modifications as previously described (Wakamatsu et al., 1986). To prepare multilamellar vesicles, a chloroform solution of DPPC-d_{80} was evaporated and suspended in a small volume of D_2O (or H_2O) at 60 °C. Afterward, the product was lyophilized to remove the residual chloroform and then resuspended in a known volume of D_2O (or H_2O). The lipid concentration was determined by a total phosphorus assay according to Bartlett (1959).

NMR Measurements. Two-dimensional (2D) proton NMR spectra were recorded on a Bruker AMX-600 spectrometer operating at 600 MHz. Chemical shifts were measured with an accuracy of ±0.01 ppm, relative to the methyl resonance of internal 4,4-dimethyl-4-silapentane-1-sulfonate. Melittin was dissolved in either 90% H_2O/10% D_2O or 99.8% D_2O. Sample pH (direct pH meter reading) was, respectively, adjusted to 3.0 with HCl or DCl, and the temperature was kept at 45 °C unless otherwise specified. Since the phase transition temperature of DPPC-d_{80} is 35.5 °C (Wakamatsu et al., 1986), the vesicles are in the liquid-crystalline phase at 45 °C.

To obtain sequential resonance assignments, we carried out 2D TOCSY (Bax & Davis, 1985) and ROESY (Bothner-By et al., 1984) on a 2 mM lipid-free melittin sample in a 90% H_2O/10% D_2O solution. Experiments were performed at 23 and 45 °C. Water resonance was eliminated by presaturation. PE-COSY (Müller, 1987) was also carried out on the same sample in a 99.8% D_2O solution. We used the States–TPPI method (Marion et al., 1989) to obtain F_1 quadrature detection. The mixing times (τ_m) were set at 200 ms for ROESY and 75 ms for TOCSY. In TOCSY and ROESY, spectral widths in both dimensions were adjusted to 5556 Hz to avoid overlap of the folded Trp^{19} indole NH proton resonance with the amide proton resonances, and data points in the t_1 and t_2 dimensions were, respectively, 512 and 2048. For PE-COSY, the spectral width in the F_1 dimension was reduced to 2778 Hz, and the data points in the t_1 and t_2 dimensions were, respectively, 1024 and 2048. In all cases, time-domain data were multiplied in both dimensions by a shifted, squared sine function and expanded by zero-filling to give 1024 × 1024 frequency domain data. NOESY experiments (Jeener et al., 1979; Macura et al., 1981) were carried out on a 2 mM melittin sample in the presence and absence of 8.1 mM DPPC-d_{80}. The TPPI method (Bodenhausen et al., 1984) was employed for quadrature detection in the F_1 dimension of the NOESY spectra. The water resonance in the 90% H_2O/10% D_2O solution was eliminated by presaturation. The τ_m in NOESY was set at 100, 200, and 300 ms, with the 100-ms setting being subsequently used to extract the distance constraints. Other experimental conditions were the same as those in ROESY and TOCSY.

Computation Procedure. Significant overlap of the melittin proton resonances made it difficult to quantify the NOE cross-peaks; hence, we set the upper and lower limits on the interproton distance for all NOE peaks at 4.0 and 2.0 Å. The variable target function distance geometry calculations in dihedral angle space (Braun & Go, 1985) were carried out using the DADAS program. For the NOEs involving methyl groups of alanine, isoleucine, and threonine, pseudoatoms were introduced at the center of mass of the three methyl protons, and a distance correction was made by adding 0.5 Å to the upper limit value and subtracting 0.5 Å from the lower limit value (Wüthrich et al., 1983). Distance constraints for leucine Cδ methyl protons, for which a stereospecific assignment could not be made, were replaced with those for a pseudoatom placed at the center of mass of the six methyl protons, and a distance correction term of 2.0 Å was added to the upper limit and subtracted from the lower limit. For methylene protons that could not be stereospecifically assigned (including those of glycines), we used pseudoatoms located at the center of mass of the methylene protons, with a distance correction term of 1.0 Å being added to and subtracted from the upper and lower limits, respectively.

DADAS was run on a DEC VS4000/60 workstation with 81 intraresidue and 108 interresidue NOE constraints. NOEs observed between spin-coupled protons were not included in the calculation. From 81 initial random structures, 29 structures were selected having a maximum distance violation less than 0.5 Å. The 29 structures were then refined with restrained molecular dynamics calculations using the XPLOR program (ver. 3.0; Brünger et al., 1987) run on a SGI IRIS 4D80GTB computer. During XPLOR calculations, interproton distances were set to 3.0 ± 1.0 Å for all NOE cross-peaks. The $(\langle r^{-6}\rangle)^{-1/6}$ distance averaging method (Clore et al., 1987) was used for equivalent protons. Distance constraints involving nonequivalent protons that could not be stereospecifically assigned were referred to the center average distance, which is similar to a pseudoatom representation. The NOE pseudopotential was described by a square-well function, and its force constant was set at 50 kcal·mol^{-1}·Å^{-2}. The force constants of bonds, angles, and improper torsions were, respectively set at 1000 kcal·mol^{-1}·Å^{-2}, 500 kcal·mol^{-1}·rad^{-2}, and 500 kcal·mol^{-1}·rad^{-2}. The improper tor-

sion potential is needed to keep the planarity of *trans* peptide bonds and aromatic rings. We neglected electrostatic interactions and used a repel energy function for the van der Waals potential (Kraulis et al., 1989). Initially, a high system temperature (2000 K) was applied, which was then decreased to 100 K in steps of 50 K. Each structure was finally energy minimized with NOE constraints. Of the 29 structures refined by XPLOR, we selected 13 structures for further analysis that did not have a distance violation larger than 0.5 Å. The average structure and structural statistics were calculated using the QUANTA program (ver. 3.3, Polygen Corp., Waltham, MA).

Model Calculation. In addition to the calculations using experimental data, we performed a similar model calculation of the structure of melittin using distance constraints obtained from tetrameric melittin in the crystal form (Terwilliger & Eisenberg, 1982). The atomic coordinates of the melittin A chain were extracted from the Protein Data Bank, and those of the hydrogen atoms were generated using CHARMm HBUILD functionality (Brooks et al., 1983). Next we picked out all the proton pairs (76 intraresidue and 105 interresidue) that are within 4.0 Å of each other. The r^{-6} averaging method was used for calculating a distance involving methyl protons. As previously mentioned, pseudoatoms were used for protons that could not be stereospecifically assigned (including $C\alpha H_2$ of glycines). Upper and lower distance bounds were, respectively, 4.0 and 2.0 Å, although some correction terms mentioned before were applied to the bounds. Starting with 51 random structures, 27 DADAS structures were refined using XPLOR, and nine structures having no distance violation larger than 0.5 Å were selected.

RESULTS

Assignment of Free (Monomeric) Melittin Proton Resonance. Under the condition of low ionic strength and low peptide concentration (≤3 mM), free melittin molecules are known to be monomeric in aqueous solution (Brown et al., 1980). Proton resonance assignments of several amino acid residues in monomeric melittin were made by Lauterwein et al. (1980), and we confirmed their results using TOCSY, as well as completely assigning the side chain resonances of all residues. We also made stereospecific assignments of Pro^{14} $C\beta$, $C\gamma$, and $C\delta$ protons by referring to the intraresidue ROEs and $^3J_{\alpha\beta}$s (Wagner et al., 1987). The $C\beta$ proton at 2.30 ppm ($H\beta^{Low}$) showed stronger ROE with $H\alpha$ than did the other $C\beta$ proton at 1.88 ppm ($H\beta^{High}$), while $^3J_{\alpha\beta}$ was larger for $H\beta^{High}$ (8.5 Hz) than for $H\beta^{Low}$ (6.8 Hz); hence, $H\beta^{High}$ and $H\beta^{Low}$ were assigned to $H\beta2$ and $H\beta3$, respectively. Because the $C\delta$ proton at 3.63 ppm ($H\delta^{High}$) showed larger ROE with the $H\beta2$ proton than did the other $C\delta$ proton at 3.85 ppm ($H\delta^{Low}$), $H\delta^{High}$ was assigned to $H\delta2$. The $C\gamma$ proton at 2.05 ppm was assigned to $H\gamma2$ since it showed larger ROE with the $C\alpha$ proton than did the other $C\gamma$ proton at 2.00 ppm.

We also performed a complete sequence-specific resonance assignment, which is not available from earlier work, based on the ROE peak observed between the $C\alpha$ proton of one residue and the amide proton of the next residue (Figure 1a). Table 1 summarizes the resultant resonance assignments of free monomeric melittin in an aqueous solution.

It should be noted that all ROE peaks observed were of either intraresidue or sequential (between neighboring residues) origin, with no medium- or long-range ROE cross-peaks being found. This observation indicates that a free melittin molecule in an aqueous solution does not take a folded conformation, a result that is consistent with a chemical shift of melittin protons, which is close to that of random coil model peptides (Lauterwein et al., 1980).

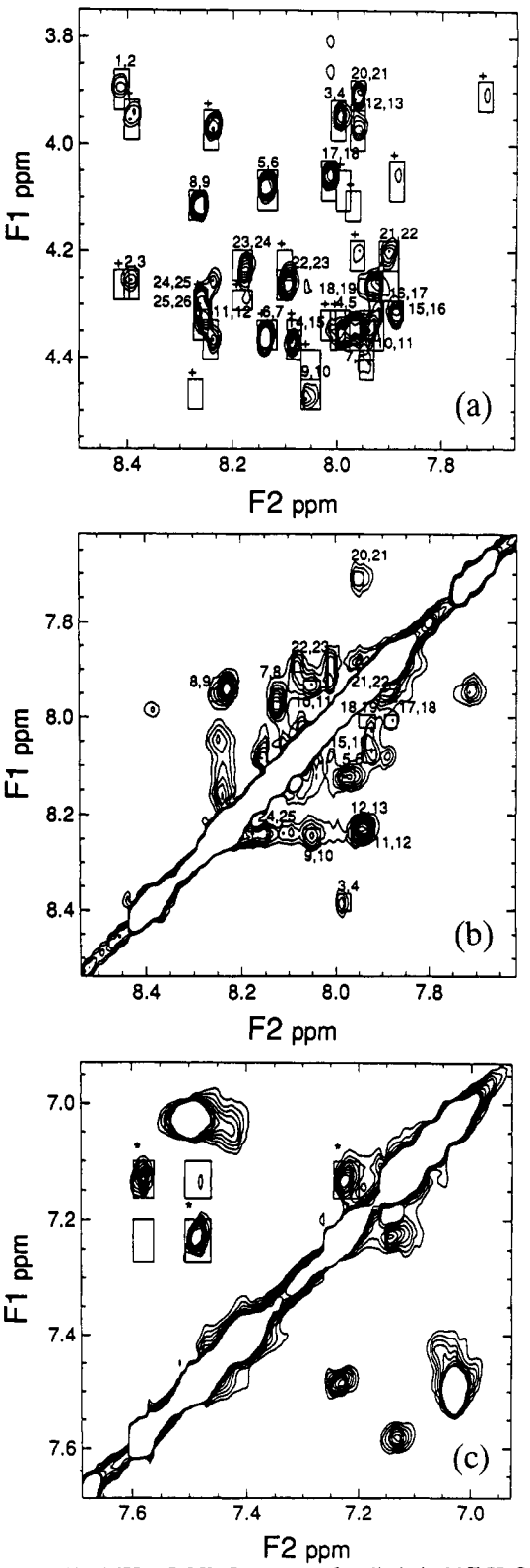

FIGURE 1: 600-MHz 2D NMR spectra of melittin in 90% H_2O/10% D_2O at pH 3.0. (a) ROESY spectrum ($C\alpha H$/NH region) in the absence of DPPC-d_{80} vesicles at 45 °C. (b and c) 2D TRNOE spectra in the presence of DPPC-d_{80} vesicles (8.1 mM) at 45 °C; (b) NH/NH and (c) aromaric/aromatic regions. Mixing times are (a) 300 ms and (b and c) 100 ms. In panels a and b, each sequential NOE peak is annotated by an open rectangle and its associated residue numbers. Intraresidue NOEs are marked with a "+" sign. In panel c, asterisks indicate TRNOE cross-peaks between close protons, while open rectangles specify positions where cross-peaks were expected between distal protons.

Table 1: Proton Chemical Shifts (ppm) of Melittin in an Aqueous Solution at pH 3.0, 45 °C

residue	NH	α	β	others
Gly[1]		3.89		
Ile[2]	8.43	4.24	1.89	γ_2 1.21, 1.36; γ_3 0.94; δ_3 0.94
Gly[3]	8.41	3.94		
Ala[4]	8.01	4.33	1.37	
Val[5]	8.00	4.07	2.05	γ_3 0.93, 0.93
Leu[6]	8.15	4.35	1.59, 1.59	γ 1.59; δ_3 0.86, 0.92
Lys[7]	8.15	4.33	1.72, 1.79	γ_2 1.44; δ_2 1.66; ϵ_2 2.97
Val[8]	7.98	4.10	2.05	γ_3 0.93, 0.93
Leu[9]	8.28	4.46	1.63, 1.63	γ 1.63; δ_3 0.87, 0.93
Thr[10]	8.07	4.40	4.27	γ_3 1.20
Thr[11]	7.96	4.36	4.25	γ_3 1.21
Gly[12]	8.25	3.95		
Leu[13]	7.95	4.59	1.62, 1.62	γ 1.62; δ_3 0.93, 0.93
Pro[14]		4.35	1.88, 2.30	γ2 2.05; γ3 2.00; δ2 3.63; δ3 3.85
Ala[15]	8.10	4.25	1.37	
Leu[16]	7.95	4.30	1.61, 1.61	γ 1.61; δ_3 0.86, 0.92
Ile[17]	7.91	4.04	1.82	γ_2 1.19, 1.44; γ_3 0.76; δ_3 0.82
Ser[18]	8.04	4.33	3.81, 3.86	
Trp[19]	7.96	4.60	3.31, 3.36	δ1 7.25; ε3 7.58; η2 7.23; ζ3 7.13; ζ2 7.48
Ile[20]	7.73	3.89	1.77	γ_2 1.10, 1.37; γ_3 0.83; δ_3 0.83
Lys[21]	7.98	4.19	1.75, 1.84	γ_2 1.38, 1.47; δ_2 1.66; ϵ_2 2.95
Arg[22]	7.91	4.25	1.76, 1.82	γ_2 1.61; δ_2 3.13; NεH 7.06
Lys[23]	8.11	4.25	1.66, 1.76	γ_2 1.38, 1.48; δ_2 1.62; ϵ_2 2.97
Arg[24]	8.18	4.28	1.77, 1.84	γ_2 1.64; δ_2 3.18; NεH 7.12
Gln[25]	8.27	4.29	2.00, 2.11	γ_2 2.37; $N\epsilon H_2$ 6.75, 7.41
Gln[26]	8.27	4.29	2.00, 2.11	γ_2 2.37; $N\epsilon H_2$ 6.75, 7.41
NH_2	7.03	7.50		

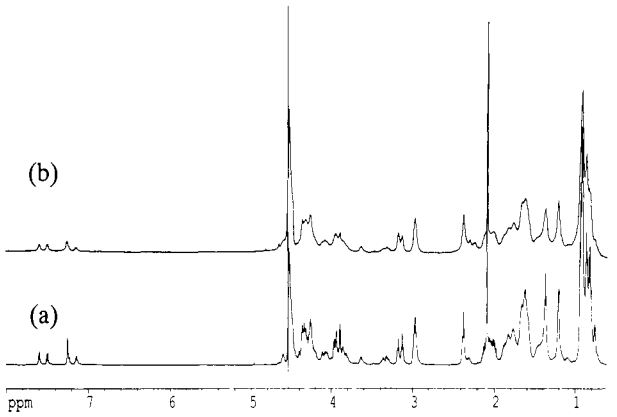

FIGURE 2: 600-MHz proton NMR spectrum of melittin (2 mM) in 99.8% D_2O in the (a) absence and (b) presence of DPPC-d_{80} vesicles (8.1 mM) at pH 3.0 and 45 °C.

NOE in the Absence of Lipid Vesicles. Because NOEs for free peptide molecules can make it difficult to interpret TRNOEs in the presence of lipid vesicles, we examined whether NOEs are observed in the absence of vesicles under the condition used for TRNOE measurements (45 °C). As expected for medium-sized linear peptides, cross-peaks observed in the NOESY spectrum were due either to chemical exchange between two NH_2 protons (Gln[25] and Gln[26]) or to the zero-quantum coherence between *J*-coupled protons, but not due to NOE interactions (data not shown). This observation assures that NOE cross-peaks observed in the presence of lipid vesicles are due to the transfer of NOEs from the vesicle-bound state.

Spectral Change of Melittin by Addition of DPPC-d_{80} Vesicles. Upon addition of 8.1 mM DPPC-d_{80} vesicles at 45 °C, the proton resonances of melittin molecules broadened without any detectable changes in the chemical shifts (Figure 2). However, at 23 °C when DPPC-d_{80} bilayer is in a gel phase, such signal broadening did not occur; hence, the observed signal broadening is not due to self-aggregation of

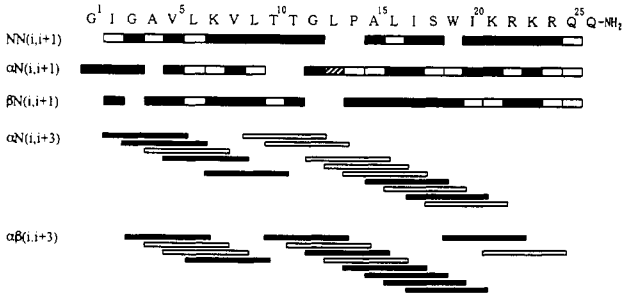

FIGURE 3: Summary of sequential and medium-range TRNOEs. TRNOE connectivities of specified proton pairs observed in the presence of DPPC-d_{80} vesicles are indicated with filled bars, while those that could not be observed due to resonance overlap are indicated with open ones. The observed TRNOE between Leu[13] NH and Pro[14] CδH is indicated with a hatched bar.

melittin molecules, but instead due to a chemical exchange between the free monomeric and vesicle-bound states. We found the exchange rate between these states to be in the slow or intermediate region on the chemical shift scale because the line width of the resonance broadened with increases in temperature (data not shown). Preliminary binding experiments monitoring Trp[19] fluorescence indicated that 5–10% of melittin molecules (2 mM) are bound to the DPPC-d_{80} vesicles (8.1 mM) under the experimental conditions used in the TRNOE measurements, being in good agreement with the NMR observation that the integrated peak intensity of free melittin signals do not significantly change upon the addition of the DPPC-d_{80} bilayer.

TRNOE of Vesicle-Bound Melittin. In the presence of DPPC-d_{80} vesicles, a large number of negative NOE peaks were observed among peptide proton resonances (Figure 1b) for almost all residues from the N- to C-terminus. These NOEs are TRNOEs due to the vesicle-bound melittin molecules, since the magnitude of the NOE increased with increases in the lipid/peptide molar ratio. NOEs involving main chain protons are summarized in Figure 3. It should be noted that the NOE pattern of melittin in the presence of DPPC-d_{80} vesicles was completely different from the NOE and ROE patterns of melittin in the absence of the vesicles (not shown), again confirming that bilayer-bound melittin takes a definite conformation and that the observed NOEs were transferred from bound peptide molecules (i.e., TRNOE) and not due to free molecules.

The problem of spin diffusion effects (Kalk & Berendsen, 1976) was circumvented as follows. In three NOESY spectra with τ_m at 100, 200, and 300 ms, the first two were qualitatively similar, whereas additional peaks emerged in the 300-ms spectrum. Thus, we selected the spectrum with τ_m = 100 ms, thereby being to sure to avoid spin diffusion in the vesicle-bound state. TRNOE cross-peaks observed in this NOESY spectrum were highly specific and only occurred between close protons; e.g., among Trp[19] indole ring protons, NOEs were observed for pairs (Hε3 and Hζ3, 2.49 Å), (Hζ3 and Hη2, 2.44 Å), and (Hη2 and Hζ2, 2.52 Å), but not for (Hε3 and Hη2, 4.34 Å) or (Hζ3 and Hζ2, 4.30 Å) (Figure 1c).

In addition to intraresidue TRNOEs, we observed medium-range TRNOE cross-peaks that are characteristic of an α-helical conformation, i.e., between CαH of the *i*th residue and CβH of the (*i*+3)th residue [$\alpha\beta(i,i+3)$], CαH of the *i*th residue and the amide proton of the (*i*+3)th residue [$\alpha N(i,i+3)$], as well as between the amide proton of the *i*th residue and that of the (*i*+1)th residue [$NN(i,i+1)$] (Figure 3). The TRNOE cross-peak observed between Pro[14] CδH and Leu[13] CαH (Figure 3) indicates that the Leu[13]–Pro[14] bond is in the *trans* conformation in the vesicle-bound state.

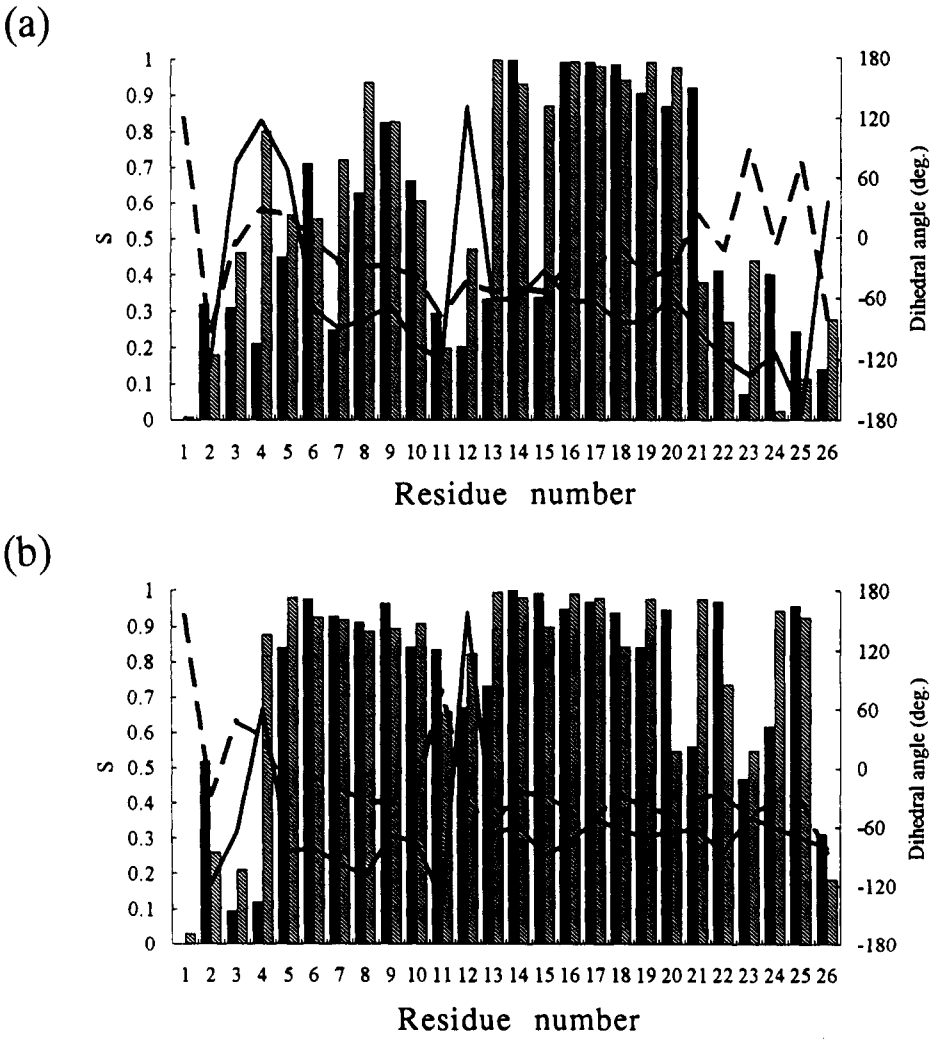

FIGURE 4: Results showing the order parameter (S) and the average value of the backbone dihedral angles (ϕ and ψ) along a melittin sequence of calculated structures using the distance constraints obtained from TRNOE spectra (a) and calculated structures using the distance data extracted from the crystal structure (b). Filled and hatched bars, respectively, show S values of ϕ and ψ angles, while solid and dashed lines, respectively, indicate the average value of ϕ and ψ.

Description of Structures. We uniformly set the upper limit on the interproton distance at 4 Å for a close proton pair between which TRNOE was observed. Although this constraint is looser than those commonly used in structure determination of proteins (Wüthrich, 1986), it proved to be enough to obtain converged structures as demonstrated by high angular order parameter (S) values for the backbone dihedral angles (ϕ and ψ) (Figure 4a). S is defined as (Detlefsen et al., 1991):

$$S = \frac{1}{N}\{(\sum_{k=1}^{N} \cos \alpha_k)^2 + (\sum_{k=1}^{N} \sin \alpha_k)^2\}, \quad (\alpha = \phi, \psi)$$

where N is the total number of successfully calculated structures. This parameter takes a value between 0 and 1, with $S = 1$ when ϕ (or ψ) is the same in all structures, whereas $S = 0$ when it is randomly distributed. In structures calculated using experimental TRNOE data, ϕ and ψ are well converged in two regions (Leu^6-Thr^{10} and Leu^{13}-Lys^{21}; Figure 4a). The regions of the N-terminal Gly^1-Val^5, C-terminal Arg^{22}-Gln^{26}, and Thr^{11}-Gly^{12}, show a low S value, hence being divergent among the calculated structures. The RMSD from the average structure for N, Cα, and C′ atoms of Leu^6-Thr^{10} and Leu^{13}-Lys^{21} was 0.53 and 0.77 Å, respectively, and the corresponding values for all non-hydrogen atoms of Leu^6-Thr^{10} and Leu^{13}-Lys^{21} were 1.36 and 1.12 Å, respectively.

(1) Region Leu^6-Thr^{10}. ϕ and ψ values of about −60° (Figure 4a) indicate that the five residues from Leu^6-Thr^{10} of vesicle-bound melittin are in an α-helical conformation in the vesicle-bound state. In this region, hydrophobic residues (Val^8 and Leu^9) are located on one side of the helix, while Lys^7 is on the other side, forming an amphiphilic helix conformation (Figure 5a).

(2) Region Leu^{13}-Lys^{21}. The C-terminal region (Leu^{13}-Lys^{21}) also forms an amphiphilic helix (Figure 5b) with hydrophobic residues on one side of the helix (Leu^{13}, Leu^{16}, Trp^{19}, and Ile^{20}), while the hydrophilic residue is on the opposite side (Ser^{18}).

(3) Arrangement of N- and C-Terminal Helices. We observed medium-range TRNOEs between Thr^{11} CβH and Pro^{14} CγH, Thr^{11} CβH and Pro^{14} Hβ2, and Val^8 CαH and Gly^{12} NH. These TRNOEs indicate that Thr^{11} and Gly^{12} are not in a regular α-helical conformation. And, because the ϕ and ψ angles of these residues did not converge in the calculated structures, their conformation is difficult to define. However, the angle between the two helix axes significantly converged ($p < 0.1$), being 86° ± 34° (mean ± SD). Note that if the helix–helix angle was uniformly distributed between 0° and 180°, the SD would be 52°. We also examined if the hydrophobic side of the N-terminal helix faces the same direction as that of the C-terminal helix, with it being found that the angle between the vector pointing from the Leu^9 Cα

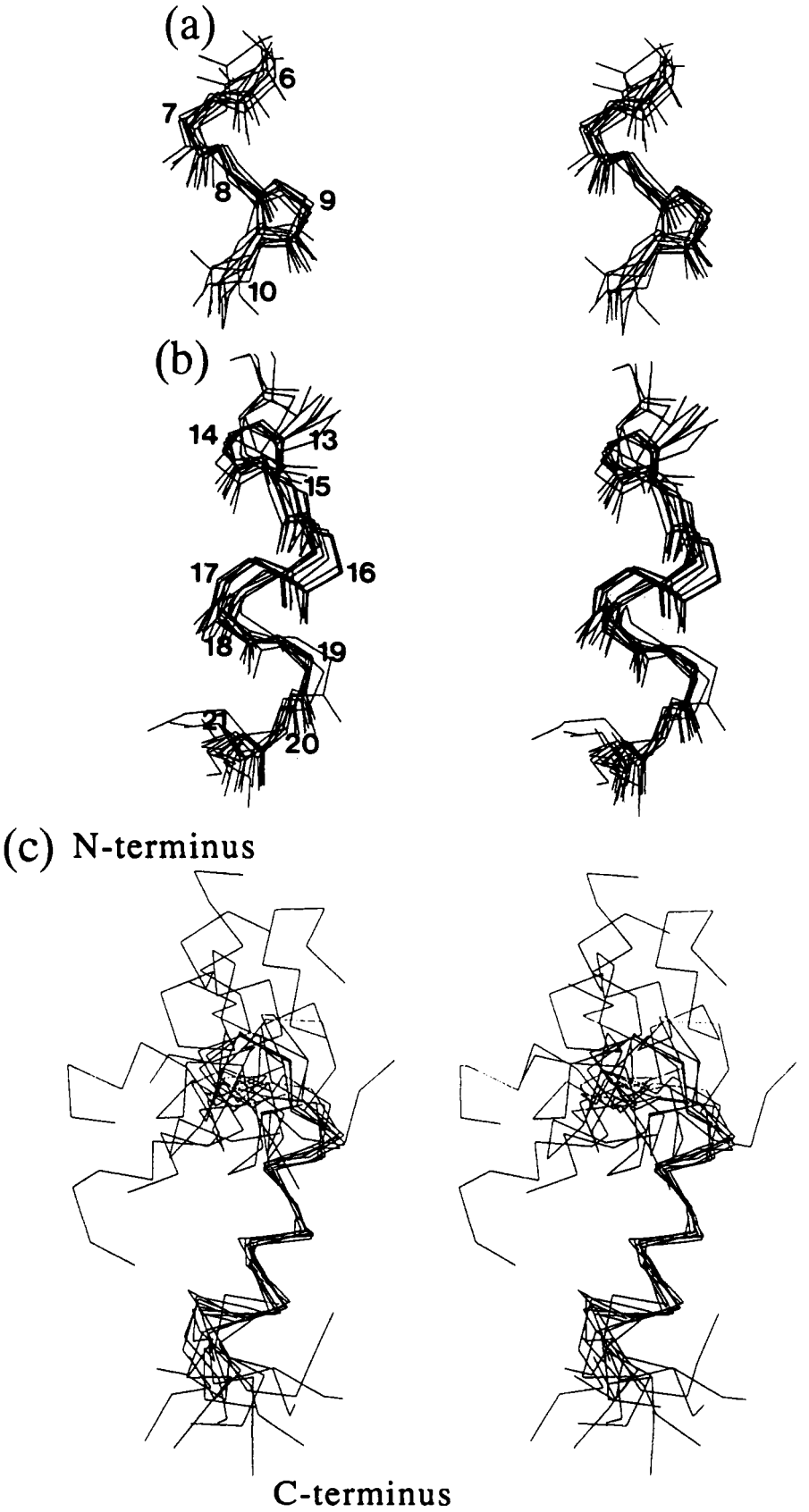

FIGURE 5: Superposition of 13 structures calculated using distance constraints obtained from TRNOE peaks in the presence of DPPC-d_{80} vesicle (stereoview). Best fit of residues Leu^6-Thr^{10} (a) and Leu^{13}-Lys^{21} (b). The whole molecule was fitted in the C-terminal helix to demonstrate the variation of the N- and C-terminal helix arrangement (c). Backbone atoms (a and b) and Cα atoms (c) are indicated.

atom to the N-terminal helix axis and the vector from the Ile^{17} Cα atom to the C-terminal helix axis is dispersed at 120° ± 41°. Leu^9 and Ile^{17} were chosen due to their resultant large S value for ϕ and ψ angles in the calculated NMR structures and also because in the crystal structure they are located on the same side of the plane defined by two helix axes [see Figure 1 of Terwilliger and Eisenberg (1982)].

Distance Geometry Calculations for the Crystal Structure. Tetrameric melittin molecules in a crystal structure are mainly α-helical with a slight bend (~120°) existing at Gly^{12}. We

performed a model calculation using distance data of the crystal structure, and the resultant structures showed good convergence and had almost the same conformation as that of the original crystal structure (Figure 4b). The RMSD determined from the average structure for N, Cα, and C′ atoms of Leu[6]-Thr[10] and Leu[13]-Lys[21] was, respectively, 0.29 and 0.42 Å, while the corresponding values for all non-hydrogen atoms of Leu[6]-Thr[10] and Leu[13]-Lys[21] were, respectively, 1.13 and 0.92 Å. Only two regions showed significant divergence, i.e., a large one at Gly[1]-Ala[4] and a slight one at Thr[11]-Leu[13]. Both regions have a glycine residue that shows only two proton signals [NH and (two) equivalent CαHs].

The angle between the two helix axes in these "crystal-simulating structures" (123° ± 24°; mean ± SD) significantly converged ($p < 0.025$) and was accurately determined since the corresponding angle of the crystal structure is 115°. This helix-helix angle is significantly larger than that of the "TRNOE structures" (86° ± 34°; $p < 0.025$). Also in contrast to the TRNOE structures, the relative orientation of two hydrophobic faces of the two helices was precisely reproduced. The angle between the vector from the Leu[9] Cα atom to the N-terminal helix axis and the vector from the Ile[17] Cα atom to the C-terminal helix axis was calculated as 54° ± 18°, whereas the corresponding angle in the melittin A chain in crystal is 74°. This angle is not close to zero because the angle contains the contribution by the helix bend angle of 64°.

The importance of this model calculation is that it assures us that an accurate structure can be obtained even when using loose interproton distance constraints without dihedral angle data. Moreover, it assists in discriminating whether the disorder found in some segments of NMR structures is indicative that the segment does not actually take a definite conformation or is due to some limitation(s) in the structure calculations.

DISCUSSION

Origin of TRNOE. Conflicting observations exist concerning the association state (monomeric vs tetrameric) and orientation (parallel, perpendicular, or wedged to the membrane surface) of melittin molecules in lipid bilayers [see review by Dempsey (1990)].

We found that all the TRNOE cross-peaks in the presence of DPPC-d_{80} vesicles are compatible with a monomeric form in the vesicle-bound state, as evidenced by small violations in the structure calculations. Moreover, the NOEs observed in aggregated melittin molecules between Ile[2] δCH_3 and Trp[19] indole protons (Brown et al., 1980) were not detected in the presence of the vesicles (data not shown). No sign of an aggregated form was detected in the present study; however, this does not exclude the possibility of aggregation in the vesicle-bound state, because the dissociation rate of vesicle-bound melittin aggregates to monomers in solution is expected to be too low (Brown et al., 1980) to contribute detectable TRNOE signals (<1 s^{-1}; Ni, 1992).

It should be noted that the trans-negative membrane potential reversibly translocates the N-terminal part of melittin molecules across a lipid membrane, thereby orienting the peptides perpendicular to the membrane surface (Kempf et al., 1982). Because no electric potential was applied in the present study, however, a perpendicular disposition of the peptides is not expected. In addition, perpendicularly disposed molecules will not contribute to the observed TRNOE because their off-rate from the membrane is too low. Moreover, magainin, an amphiphilic peptide which lyses mammalian cells (Cruciani et al., 1991) and uncouples respiration from energy-producing processes (Westerhoff, 1989), has been shown to lie in the lipid bilayer with its helix axis parallel to the bilayer surface (Bechinger et al., 1992). Still, the possibility remains that the observed TRNOEs are due to peptide molecules that are wedged in a bilayer surface and whose off rate is not so low to prevent TRNOE detection. In contrast to melittin, mastoparan-X, a 14-residue amphiphilic peptide from wasp venom, showed TRNOE in the presence of DPPC-d_{80} vesicles *in the gel phase* (Wakamatsu et al., 1992). Such different behaviors indicate that the off-rate from vesicles of melittin is slower than that of mastoparan-X. Since the structure of vesicle-bound mastoparan-X was found to be one amphiphilic, straight α-helix except for the two N-terminal residues, the slower off-rate of melittin may be due to the hypothesized wedge-like disposition in a membrane. To clarify this, the detailed orientation of a melittin molecule in a bilayer will be analyzed by quenching of TRNOEs by spin-labels specifically introduced at various depths of a bilayer (Wakamatsu et al., 1987).

Melittin is known to perturb a bilayer structure of phospholipids (Sessa et al., 1969; Dufourc et al., 1986), yet under our experimental conditions, the bilayer structure of DPPC-d_{80} is considered to be retained, i.e., TRNOE cross-peaks were only observed at a temperature above the phase transition temperature of the phospholipid. This is noteworthy to mention because such behavior is not expected for micellar phospholipids. Melittin is known to promote fragmentation of the lipid bilayer of saturated phosphatidylcholine in a gel phase (Dufourc et al., 1986). However, no new resonances emerged upon the addition of DPPC-d_{80} vesicles in the gel phase, eliminating the possibility of micelle formation by melittin molecules. In addition, electron microscopy studies by Sessa et al. (1969) and us (taken of the same sample used for NMR; data not shown) have proven that the bilayer structure is retained in the presence of melittin.

Less-Ordered Structure in the N- and C-Termini and the Hinge Region. In structures calculated using experimental TRNOE data, the N- and C-termini (Gly[1]-Val[5] and Arg[22]-Gln[26], respectively) and the hinge segment (Thr[11]-Gly[12]) are less ordered than the rest of the molecule as shown in Figure 4a. We believe that the C-terminal and hinge regions do not take a definite structure in the vesicle-bound state because only a few interresidue TRNOE cross-peaks were observed in C-terminal several residues (Figure 3) and because in these regions smaller values of the order parameter were obtained for NMR structures than for the "crystal-simulating structures" (Figure 4b). On the other hand, regarding the N-terminal, the lack of convergence in a few residues of vesicle-bound melittin (Figures 4a and 5c) does not necessarily indicate that the N-terminal part is not in an ordered conformation in the vesicle-bound state, because the distance constraints extracted from melittin's crystal structure failed to give converged structures in the N-terminal (Figure 4b). The divergence in this region is ascribed to the equivalence of two CαHs in two glycine residues (Gly[1] and Gly[3]) that makes distance constraints in this region looser and fewer than in other regions. Supporting this postulation is the fact that the N-terminal region is better-defined in melittin molecules in methanol solution (Bazzo et al., 1988) or in dodecylphosphocholine micelles (Inagaki et al., 1989), where the glycines' two CαH signals have been separately observed.

Structure of Melittin in Various Environments. Listed as follows are the similarities and differences among melittin structures in crystal (Terwilliger & Eisenberg, 1982), methanol

solution (Bazzo et al., 1988), dodecylphosphocholine micelles (Inagaki et al., 1989; Ikura et al., 1991), and DPPC-d_{80} vesicles.

(1) Under all conditions, melittin has two α-helical regions that are connected via a less structured Thr[11]-Gly[12] segment.

(2) The helix bend angle varies with respect to the environment, i.e., in crystal (A chain) 114°, methanol about 160°, micelles 135° ± 15°, and vesicles 86° ± 34°. In the crystal structure with the 114° bend, two hydrophobic sides face the same "inner" direction. Because such a distribution of hydrophobic residues is not compatible with a flat phospholipid bilayer, a rotation must occur about the backbone dihedral angles of the Thr[11]-Gly[12] hinge, thereby explaining why the different helix bend angles are present in crystal and vesicles.

(3) The C-terminal Arg[22]-Gln[26] segment is in an α-helical conformation in crystal, methanol, and micelles, whereas this segment does not take an ordered conformation in vesicles, this being the most striking difference distinguishing the vesicle-bound conformation from that of the others. Were the Arg[22]-Gln[26] segment to take an α-helical structure in the vesicle-bound state, the cationic side chains of Lys[23] and Arg[24] would be buried in the hydrophobic interior of lipid bilayer; an energetically quite unfavorable situation. In agreement with this observation, an amide exchange analysis on melittin molecules bound to bilayers of phosphatidylcholine and phosphatidylserine has shown that the four C-terminal residues are not involved in an α-helical conformation (Dempsey & Butler, 1992).

(4) Residues Trp[19] and Ile[20] are in a regular α-helix in the vesicle-bound state (Figure 4a) and crystal, whereas the ϕ and ψ angles of these residues deviate from normal α-helical values in the micelle-bound state (Ikura et al., 1991).

(5) Conformations of several side chains differ depending on the environments: the strong NOEs observed between Trp[19] ring protons and Lys[23] CϵH2 in a micelle-bound melittin molecule were not detected in the vesicle-bound one (Figure 6a), whereas the TRNOE between Lys[21] CϵH$_2$ and Ile[17] Cγ2CH$_3$ was only observed in vesicle-bound melittin (Figure 6b).

Our study is the first report to clearly show that a peptide's conformations are not always the same in the vesicle- and the micelle-bound states. Though we can expect the absence of the regular α-helix in the C-terminus of vesicle-bound melittin molecule, it is difficult to imagine that the helix bend angle is less in the vesicle-bound state than in the micelle-bound state; hence a peptide's vesicle-bound conformation must be experimentally determined in order to investigate the interaction of the peptide with phospholipid vesicles. We believe our TRNOE method in the presence of perdeuterated phospholipid vesicles is best suited for this purpose.

Structure–Activity Relationship. The determined vesicle-bound conformation of melittin was found to better explain the lytic activity of the peptide and its analogs than do the conformations in crystal or the vesicle-bound state. Blondelle and Houghten (1991) showed that a single-residue deletion of Thr[10], Thr[11], Gly[12], Lys[21], Arg[22], Lys[23], Arg[24], Gln[25], or Gln[26] does not affect melittin's lytic activity, whereas a single-residue deletion at other sites reduces it. The sites tolerant toward single-residue deletion coincide with regions that do not take an ordered conformation in the vesicle-bound state. Such a clear coincidence showing that important activity-related residues are in an α-helical conformation and vise versa is much less prominent in crystal and in the micelle-bound state where residues Lys[21]-Gln[26] are involved in an α-helix. The structure–activity relationship elucidated in this study is also compatible with earlier reports that showed that the C-terminal positive charges are crucial for the peptide's lytic activity (Habermann & Jentsch, 1967; Schröder et al., 1971). Interaction of C-terminal basic residues with DPPC-d_{80} vesicles as evidenced by the presence of sequential NOEs (Figure 3) and intraresidue NOEs (not shown) may well serve to anchor the melittin molecule to vesicles via ionic interactions.

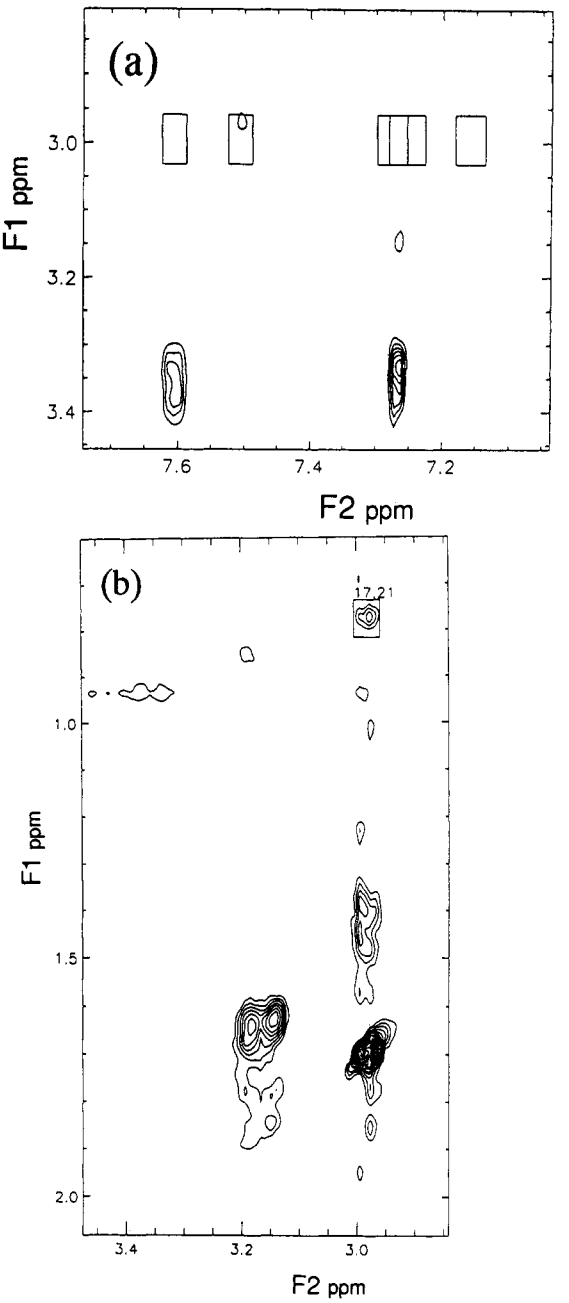

FIGURE 6: TRNOE cross-peaks characteristic of vesicle-bound melittin; aliphatic/aromatic region (a) and aliphatic/aliphatic region (b). For micelle-bound melittin, NOE cross-peaks were observed between Trp[19] indole protons and Lys[25] CϵH$_2$ (Inagaki et al., 1989). In panel a, the rectangles indicate positions in vesicle-bound melittin where the corresponding NOE cross-peaks should appear but were not observed. In panel b, the TRNOE cross-peak between Lys[21] CϵH$_2$ and Ile[17] Cγ2 CH$_3$ is annotated by the pair of residue numbers.

We have demonstrated that it is possible to obtain detailed information on the structure of melittin molecules in the vesicle-bound state using TRNOE experiments in the presence of perdeuterated phospholipid vesicles. Our unique and powerful approach showed that a peptide can take different conformations in vesicles and micelles and that the activity of melittin is better related to the conformation in vesicles than that in

micelles or methanol. Thus, research directed at elucidating structure–activity relationships of membrane-active compounds should use a vesicle-bound conformation rather than a micelle-bound one.

ACKNOWLEDGMENT

Sincere gratitude is extended to Professor Terumi Nakajima and Dr. Tadashi Yasuhara, Tokyo Medical and Dental University, for their valuable advice on melittin purification, and to Professor Masako Oosumi, Japan Women's University, for electron micrographs of phosphatidylcholine vesicles in the presence of melittin.

REFERENCES

Albrand, J. P., Birdsall, B., Feeney, J., Roberts, G. C. K., & Burgen, A. S. V. (1979) *Int. J. Biol. Macromol. 1*, 37–41.
Bartlett, G. R. (1959) *J. Biol. Chem. 234*, 466–468.
Bax, A., & Davis, D. G. (1985) *J. Magn. Reson. 65*, 393–402.
Bazzo, R., Tappin, M. J., Pastore, A., Harvey, T. S., Carver, J. A., & Campbell, I. D. (1988) *Eur. J. Biochem. 173*, 139–146.
Bechinger, B., Zasloff, M., & Opella, S. J. (1992) *Biophys. J. 62*, 12–14.
Blondelle, S. E., & Houghten, R. A. (1991) *Biochemistry 30*, 4671–4678.
Bodenhausen, G., Kogler, H., & Ernst, R. R. (1984) *J. Magn. Reson. 58*, 370–388.
Bothner-By, A. A., Stephens, R. L., Lee, J., Warren, C. D., & Jeanloz, R. W. (1984) *J. Am. Chem. Soc. 106*, 811–813.
Braun, W., & Go, N. (1985) *J. Mol. Biol. 186*, 611–626.
Brooks, B., Bruccoleri, R., Olafson, B., States, D., Swaminathan, S., & Karplus, M. (1983) *J. Comput. Chem. 4*, 187–217.
Brown, L. R., Lauterwein, J., & Wüthrich, K. (1980) *Biochim. Biophys. Acta 622*, 231–244.
Brown, L. R., Braun, W., Kumar, A., & Wüthrich, K. (1982) *Biophys. J. 37*, 319–328.
Brünger, A. T., Kuriyan, J., & Karplus, M. (1987) *Science 235*, 458–460.
Campbell, A. P., & Sykes, B. D. (1991) *J. Magn. Reson. 93*, 77–92.
Clore, G. M., & Gronenborn, A. M. (1982) *J. Magn. Reson. 48*, 402–417.
Clore, G. M., Gronenborn, A. M., Nilges, M., Sukumaran, D. K., & Zarbock, J. (1987) *EMBO J. 6*, 1833–1842.
Cruciani, R. A., Barker, J. L., Zasloff, M., Chen, H.-C., & Colamonici, O. (1991) *Proc. Natl. Acad. Sci. U.S.A. 88*, 3792–3796.
Dempsey, C. E. (1990) *Biochim. Biophys. Acta 1031*, 143–161.
Dempsey, C. E., & Butler, G. S. (1992) *Biochemistry 31*, 11973–11977.
Detlefsen, D. J., Thanabal, V., Pecoraro, V. L., & Wagner, G. (1991) *Biochemistry 30*, 9040–9046.
Dufourc, E. J., Smith, I. C. P., & Dufourcq, J. (1986) *Biochemistry 25*, 6448–6455.
Habermann. E. (1972) *Science 177*, 314–322.
Habermann, E., & Jentsch, J. (1967) *Hoppe-Seyler's Z. Physiol. Chem. 348*, 37–50.
Hider, R. C. (1988) *Endeavour 12*, 60–65.
Ikura, T., Go, N., & Inagaki, F. (1991) *Proteins: Struct., Funct., Genet. 9*, 81–89.
Inagaki, F., Shimada, I., Kawaguchi, K., Hirano, M., Terasawa, I., Ikura, T., & Go, N. (1989) *Biochemistry 28*, 5985–5991.
Jeener, J., Meier, B. H., Bachman, P., & Ernst, R. R. (1979) *J. Chem. Phys. 71*, 4546–4553.
Kalk, A., & Berendsen, H. J. C. (1976) *J. Magn. Reson. 24*, 343–366.
Kempf, C., Klausner, R. D., Weinstein, J. N., Van Renswoude, J., Pincus, M., & Blumenthal, R. (1982) *J. Biol. Chem. 257*, 2469–2476.
King, T. P., Sobotka, A. K., Kochoumian, L., & Lichtenstein, L. M. (1976) *Arch. Biochem. Biophys. 172*, 661–671.
Kingsley, P. B., & Feigenson, G. W. (1979) *Chem. Phys. Lipids 24*, 135–147.
Kraulis, P. J., Clore, G. M., Nilges, M., Jones, T. A., Pettersson, G., Knowles, J., & Gronenborn, A. M. (1989) *Biochemistry 28*, 7241–7257.
Lad, P. L., & Shier, W. T. (1980) *Arch. Biochem. Biophys. 204*, 418–424.
Lauterwein, J., Brown, L. R., & Wüthrich, K. (1980) *Biochim. Biophys. Acta 622*, 219–230.
Macura, S., Hyang, Y., Suter, D., & Ernst, R. R. (1981) *J. Magn. Reson. 43*, 259–281.
Marion, D., Ikura, M., Tschudin, R., & Bax, A. (1989) *J. Magn. Reson. 85*, 393–399.
Mollay, C., & Kreil, G. (1974) *FEBS Lett. 46*, 141–144.
Müller, L. (1987) *J. Magn. Reson. 72*, 191–196.
Ni, F. (1992) *J. Magn. Reson. 96*, 651–656.
Schröder, E., Lübke, K., Lehmann, M., & Beets, I. (1971) *Experientia 27*, 764–765.
Sessa, G., Freer, J. H., Colacicco, G., & Weissmann, G. (1969) *J. Biol. Chem. 244*, 3575–3582.
Terwilliger, T. C., & Eisenberg, D. (1982) *J. Biol. Chem. 257*, 6016–6022.
Vogel, H. (1981) *FEBS Lett. 134*, 37–42.
Wagner, G., Braun, W., Havel, T. F., Shaumann, T., Go, N., & Wüthrich, K. (1987) *J. Mol. Biol. 196*, 611–639.
Wakamatsu, K., Higashijima, T., Fujino, M., Nakajima, T., & Miyazawa, T. (1983) *FEBS Lett. 162*, 123–126.
Wakamatsu, K., Okada, A., Suzuki, M., Higashijima, T., Masui, Y., Sakakibara, S., & Miyazawa T. (1986) *Eur. J. Biochem. 154*, 607–615.
Wakamatsu, K., Okada, A., Miyazawa, T., Masui, Y., Sakakibara, S., & Higashijima, T. (1987) *Eur. J. Biochem. 163*, 331–338.
Wakamatsu, K., Okada, A., Miyazawa, T., Ohya, M., & Higashijima, T. (1992) *Biochemistry 31*, 5654–5660.
Westerhoff, H. V., Juretic, D., Hendler, R. W., & Zasloff, M. (1989) *Proc. Natl. Acad. Sci. U.S.A. 86*, 6597–6601.
Wüthrich, K. (1986) *NMR of Proteins and Nucleic Acids*, Wiley, New York.
Wüthrich, K., Billeter, M., & Braun, W. (1983) *J. Mol. Biol., 169*, 949–961.